HEFAT2012
9th International Conference on Heat Transfer, Fluid Mechanics and Thermodynamics
16 – 18 July 2012
Malta

CFD OF A HYBRID COOLING SYSTEM COMPOSED OF A DISPLACEMENT VENTILATION UNIT AND A RADIANT COOLING FLOOR

Peña-Suárez J.M. and Ortega-Casanova J.*
*Author for correspondence
Department of Mechanical Engineering and Fluid Mechanics,
University of Málaga,
Málaga,
Spain,
E-mail: jortega@uma.es

ABSTRACT

The combined use of displacement ventilation (DV) [1-2] and a radiant cooling floor (RCF) [3-5] is increasingly common in the field of building climatization. DV systems are based on injecting air directly into the occupied zone of the building, at low speed and at a temperature slightly below the comfort one. On the other hand, RCF systems are based on circulating cold water through a circuit of pipes embedded in the pavement.

With this hybrid cooling system (DV+RCF) that combines both technologies [6], only the occupied zone is climatizated and a vertical stratification of the room air temperature is achieved [7]. In addition, indoor air quality is greater than when conventional cooling systems are used [8], because the updraft convection currents caused by heat sources in the occupied zone [9], move the hot air and contaminants to the roof level going through the occupied zone only once.

DV+RCF systems work better in building with high ceiling (of 3 meters high or more), where the air stratification will improve the thermal efficiency and pollution control. Therefore, its use is appropriate in large public buildings, for example theatres [10], museums [11], train stations [12] or airport terminals [13], which are characterized by their high rise.

Despite the advantages of implementing a DV+RCF system, their behaviour is not well characterized for an efficient dimensioning of the system. Therefore, the aim of this paper is to present two correlations to quantify, on the one hand, the amount of energy (as heat) the floor is able to absorb by convection, that is, the heat flux along the floor, and, on the other hand, the maximum distance of influence of the primary air stream driven by the DV system. These correlations have been found for the hybrid cooling system DV+RCF in a large enclosure, using computational fluid dynamics (CFD). Moreover, they take into account the presence of the cooling floor and the vertical stratification of air temperature in the enclosure, becoming a powerful tool to help in the cooling system dimensioning. Multiple simulations with different Reynolds, based on the size of the diffuser and its supply air flow rate, and Grashof, based on the temperature difference between the floor and the air supplied by the diffuser, numbers were used to obtain the correlations.

NOMENCLATURE

v^*	[-]	Dimensionless velocity
v_s	[m/s]	Mean air velocity at the diffuser exit
$\lvert v \rvert$	[m/s]	Magnitude of the air velocity
v_{max}	[m/s]	Maximum velocity in the velocity profile
A_e	[m^2]	Total area of the enclosure
A_l	[m^2]	Lateral area of the diffuser
A_{eff}	[m^2]	Effective discharge area of the diffuser
K	[-]	Percent of the diffuser lateral area considered as effective area
h	[m]	Height of the diffuser
D	[m]	Outer diameter of the diffuser
δ	[m]	Height where $\lvert v \rvert = 0.5\ v_{max}$
$\dot{V}_s$	[m^3/h]	Air flow rate supplied by one diffuser
N_d	[-]	Number of diffusers
$\dot{V}_t$	[m^3/h]	Total air flow rate
Γ	[-]	Dimensionless temperature
T	[ºC]	Air temperature in the enclosure
T_s	[ºC]	Air temperature supplied by the diffuser
T_f	[ºC]	Floor temperature
R_{occup}	[m^2/person]	Occupancy rate of the enclosure
Re	[-]	Reynolds number
Gr	[-]	Grashof number
L_c	[m]	Characteristic length of the diffuser
ΔT_{s-f}	[ºC]	Temperature difference between the air supplied by the diffuser and the floor surface
ΔT_{i-s}	[ºC]	Temperature difference between the indoor air in the occupied zone and the air supplied by the diffuser

g	[m/ s^2]	Gravity acceleration
$D_{influence}$	[m]	Maximum distance of influence of a diffuser
$A_{influence}$	[m]	Influence area of all diffusers
q_{const}	[W/ m^2]	Constant convective heat flux
$Q_{cool\ peak}$	[W]	Cooling peak load
[r, θ, z]	[m, -, m]	Cylindrical coordinates

Special characters

ρ	[kg/m^3]	Air density
μ	[kg/mK]	Air dynamic viscosity
ν	[m^2/s]	Air kinematic viscosity
C_p	[J/kgK]	Air specific heat
β	[1/C°]	Coefficient of thermal expansion

Subscripts

s	Supply
f	Floor
e	Enclosure
l	Lateral
eff	Effective
$occup$	Occupancy
c	Characteristic
t	Total
d	Diffuser
i	Indoor

INTRODUCTION

In industrialized countries, 90% of time is spent indoors where more than 40% of total energy is consumed. The air conditioning has become into the first service in terms of energy consumption in a building, being then evident that optimizing the processes of air-conditioning in buildings result in reductions in energy consumption without compromising the thermal comfort.

One way to approach the study of a particular climate control system is by CFD (Computational Fluids Dynamics). The ability to solve air-conditioning building problems using CFD is evident in studies carried out in large rooms or public places such as lecture theatres [10], museums [11], train stations [12], airport terminals [13] or classrooms [14]. More specifically, CFD has been used in the design and evaluation of both the thermal comfort and air quality in public buildings located throughout the world, such as the Yoyogi National Stadium (Japan) [15], the Galatsi Arena Stadium (Greece) [16], the lecture theatre at Hong Kong University of Science and Technology (China) [17], the Building A, located on the BP Sunbury campus (United Kingdom) [18], the Terminal 1 of Chengdu Shuangliu International Airport (China) [19] or the New Bangkok International Airport (Thailand) [20].

One of the typical architectonic features of large public buildings is their high rise. Considering that indoor thermal comfort conditions must be guaranteed just in the occupied zone (the part of the enclosure up to 1.8 m above the floor), it is possible to increase the energy efficiency of the air conditioning systems of these buildings by using a hybrid system of refrigeration composed of a radiant cooling floor, based on circulating cold water through a pipe circuit embedded in the pavement [21~24], coupled with a displacement ventilation system, based on supplying air directly into the occupied zone at low speed and at a temperature slightly below the comfort one [25-26].

The advantage of this hybrid system is the exclusive treatment of the occupied zone, achieving a vertical stratification of air temperature in the enclosure. In addition, indoor air quality is greater than that achieved with conventional cooling systems, because the upward convection currents from heat sources move the hot air and contaminants to the roof level going only once through the occupied zone. Moreover, energy savings are also achieved because the temperature of the working fluids (air in the displacement ventilation system and water in the radiant cooling floor) are close to comfort ones so energy losses in the fluid conductions are minimal.

This paper presents the application of CFD to calculate air-flow velocities and temperatures in high rise enclosures in order to obtain correlations which help to dimension the air conditioning systems of the enclosure. The velocities and temperatures numerically calculated can also be used to determine the main thermal comfort index, according to ISO 7730 [27] and, subsequently, used to obtain the thermal classification of the enclosure [28].

GEOMETRY UNDER STUDY, COMPUTATIONAL DOMAIN AND BOUNDARY CONDITIONS

It aims to analyze numerically the thermal behaviour of a cooling system based on a radiant floor, combined with cylindrical displacement diffusers, uniformly distributed in a large diaphanous enclosure, as shown in Figure 1, where a simple schematic of the cooling system under study is depicted. To that end, the numerical simulations are performed with the commercial CFD software FLUENT [29].

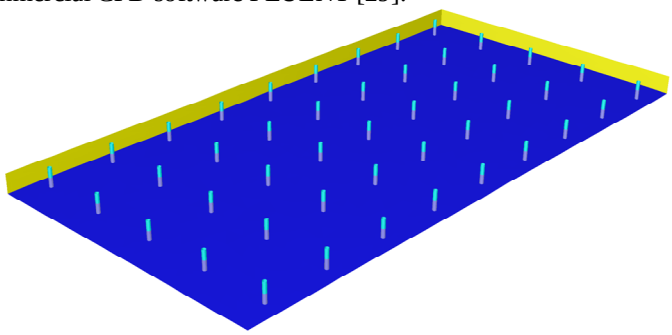

Figure 1 Displacement diffusers uniformly distributed in a large diaphanous enclosure

The three-dimensional (3D) numerical study of the enclosure, together with the diffusers, is very complex because of the large size of the domain and the high number of diffusers that must be used. However, since each diffuser has its own zone of influence around it (see Figure 2), to analyze the behaviour of the whole installation only that zone will be studied, instead of the whole and complex domain. In addition to this, simulations can be considered as two-dimensional axisymmetric, if the diffuser is seen as a cylindrical body and one takes into account its azimuthal symmetry. Therefore, the simulations could be performed on a vertical plane placed parallel to the airflow stream, as shown in Figure 3 where the

diffuser, its zone of influence (delimited by a red cylinder) and the computational plane (the black rectangle) are shown. This plane should extend from the floor to the ceiling of the enclosure (8 m wide and 8 m high) but, in order to reduce the computational time, the height of the computational domain could be halved (8 m wide and 4 m high), solved both planes numerically and their solutions compared, specially in the occupied zone (it must be noted that a special boundary condition, imposed by means of a Fluent UDF, must be used at the top boundary of the half plane). A good agreement of the numerical solutions in both planes would mean that the smallest one could be used. Both planes have been numerically simulated under the same conditions and their comparison is shown in Figure 4, where vertical profiles of $|v|$ and T are depicted at r = 4 m. As one can see, the agreement in temperature is quite good, while in velocity some divergence exists around the upper boundary condition. However, since the agreement in the occupied zone is very good, the halved plane will be studied numerically to obtain from the numerical solutions the correlations we are looking for. The main benefit of this consideration will be a reduction in the computational cost of the simulations, fact that will allow to generate more accurate grids with a high node density in certain regions of interest.

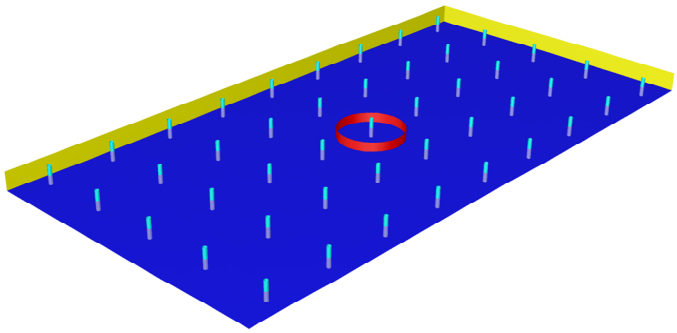

Figure 2 Zone of influence of a diffuser

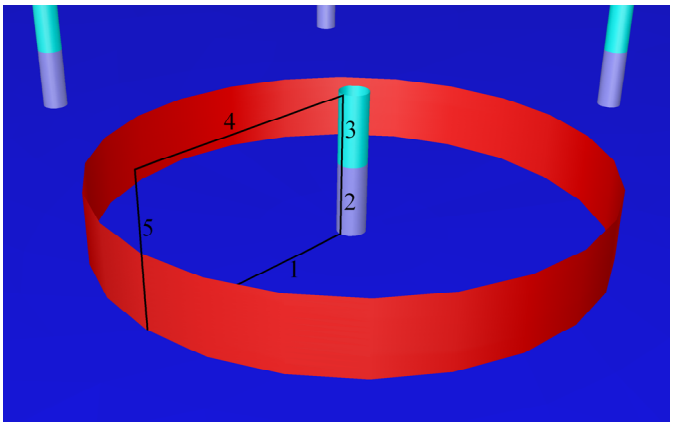

Figure 3 Close view of the zone of influence around a diffuser. The black rectangle is the computational domain. The numbers indicate different boundary conditions

The diffuser under study is a commercial one with a height (h) of 2 m high and a diameter (D) of 0.81 m. The appropriate description of air diffusers used in displacement ventilation is very difficult in CFD because of the external plate perforations. Its modelling then requires a large number of nodes to adequately capture the velocity profiles in each hole, but this would be a great inconvenience to expedite simulations. However, a certain distance downstream the diffuser, the perforations have no influence on the flow, as shown in Figure 5, where a comparison of the dimensionless velocity along vertical lines is shown in 4 radial locations when two different diffusers are used: one with perforations and the other without them. As it will be shown, around 5 cm downstream the diffusers the velocities are almost the same. The dimensionless velocity used in the comparison is defined as

$$v^* = \frac{|v|}{v_s \dfrac{A_{eff}}{A_l}}, \qquad (1)$$

where A_{eff} is the effective area of the lateral face the air goes through, and A_l is the total area of that face. In the diffuser with no perforations A_{eff} is equal to A_l. Therefore, in Figure 5, on the one hand, the solid lines correspond to a diffuser with the lateral plate cut in strips of 1 cm, thus, alternately, it supplies air or not in order to simulate the effect of the perforated plate. While, on the other hand, the dotted lines correspond to a diffuser whose lateral face is completely of air discharge. As it can be seen in Figure 5, 5 cm downstream the diffuser, the oscillations produced by the perforations are dimmed and the profiles obtained using both diffusers are quite similar. Therefore, using the diffuser without perforations the computational cost will be reduced and the results will be practically the same than when a perforated diffuser is used. So, the computational cost is reduced using a diffuser whose lateral face is completely discharging air.

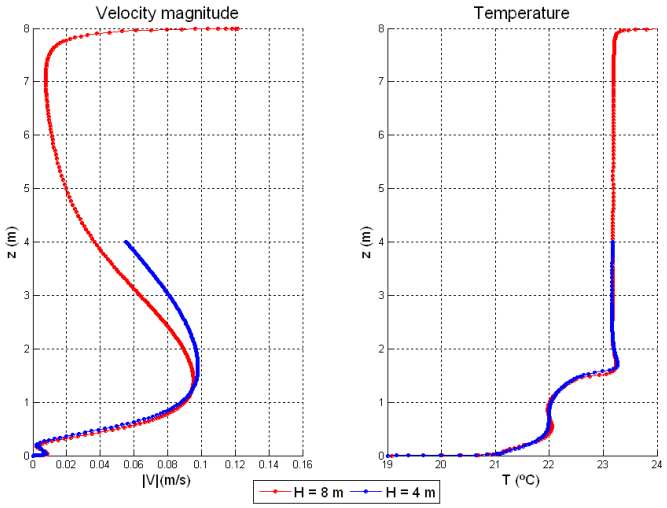

Figure 4 Comparison of the vertical profile of the velocity magnitude (left) and temperature (right) in enclosures with different height.

A structured mesh of quadrilaterals elements is used in the simulations. The elements are compressed in the region close to the floor to properly resolve the boundary layer. The grid

independence was examined by solving the flow field using three different mesh configurations with 15,476, 45,441 and 84,992 cells. Practically, the same results were obtained with the two finer meshes. On the other hand, since the quality of the mesh plays an important role in the stability and accuracy of numerical calculations, it is necessary to reach a compromise between accuracy and computational cost. Therefore, the mesh of 45,441 cells is chosen for the simulation: the use of the finest mesh only would increase the computational time.

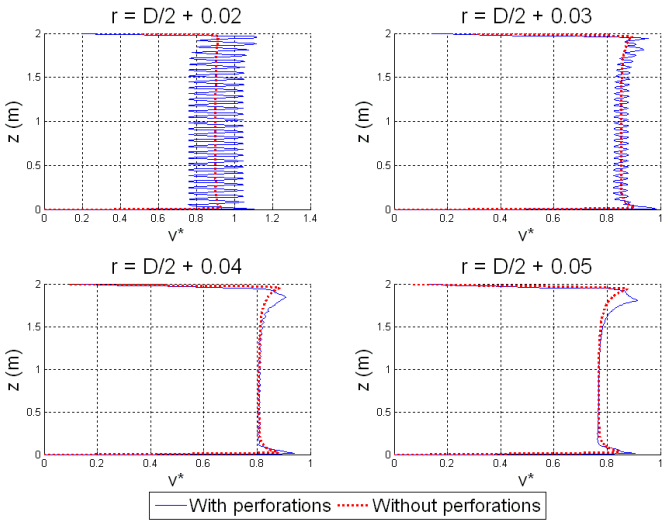

Figure 5 Dimensionless profile of the velocity magnitude along vertical lines in the radial positions indicated

Regarding the boundary conditions used in the simulations, they are described in detail in Table 1. The location of the corresponding boundary condition can be checked in the sketch of the computational domain shown in Figure 3.

1: Floor	-Type: wall -Area: 221.419 m^2 -Temperature: 20ºC -Density: 2,500 kg/m^3 -Specific heat: 1,000 J/kg K -Thermal conductivity: 2.3 W/m K
2: Supply	-Type: mass-flow-inlet -Area: 5.089 m^2 -Mass flow-rate: 1.191, 1.361 and 1.531 kg/s -Temperature: 21, 22 and 23ºC -Direction: normal to boundary -Turbulence intensity: 4.49, 4.41 and 4.35% -Hydraulic Diameter: 2,256 m
3: Air tube connection	-Type: wall -Area: 5.089 m^2 -Heat flux: 0 W/m^2 (adiabatic) -Density: 2,719 kg/m^3 -Specific heat: 871 J/kg K -Thermal conductivity: 202.4 W/m K
4: Exhaust	-Type: pressure-outlet -Area: 221.419 m^2 -Gauge pressure: 0 Pa
	-Backflow total temperature: UDF - Backflow Direction: from neighboring cell
5: Symmetry	-Type: symmetry -Area: 211.241 m^2

Table 1 Boundary condition

PHYSICAL AND NUMERICAL CONSIDERATIONS

The airflow pattern and temperature distribution in the enclosure are governed by the conservation laws of mass, momentum and energy. The flow is assumed to be axisymmetric, steady-state and turbulent with buoyancy effects taken into account. The radiation heat transfer was not included in the model. The air was modelled as an ideal gas.

Regarding the turbulent model, the two-equation k-ε RNG (Re-Normalization Group) model [30] was employed in this study. This model is a very reliable and a commonly used CFD model for assessment of indoor thermal conditions, as well as it has been used to simulate the thermal environment in large space buildings [31] where good agreement between numerical and experimental results were found. Finally, Upwind Second-Order scheme and SIMPLE algorithm were used for space discretization and coupling between pressure and velocity in the numerical simulations, respectively.

CASES STUDIES

In order to find the above mentioned correlations, on the one hand, of the amount of energy as convective heat the floor is able to absorb, that is, the heat flux along the floor, and, on the other one, of the maximum distance of influence of the displacement ventilation diffuser, 9 simulations are scheduled. They are parameterized through the air flow rate $\dot{V}_s$ supplied by the diffuser and its temperature T_s. The occupancy rate R_{occup} of the enclosure is set to 3.75 m^2/person while the floor surface is kept at a constant temperature T_f of 20 °C. Others occupancy rates and floor temperatures are going to be studied but they are still not ready. Therefore, the problem is characterized by three dimensionless parameters: Reynolds number, Grashof number and a temperature ratio defined, respectively, as

$$Re = \frac{\rho\, v_s\, L_c}{\mu}\ , \tag{2}$$

$$Gr = \frac{g\,\beta\,\Delta T_{s-f}\,L_c^3}{v_s^2}\ , \tag{3}$$

$$T = \frac{T_s}{T_f}\ . \tag{4}$$

The characteristic length (L_c) of the problem is related to the effective area of the diffuser as

$$L_c = \left(A_{eff}\right)^{1/2} = \left(K\,2\pi\,\frac{D}{2}h\right)^{1/2}\ , \tag{5}$$

that takes both the height and the diameter of the diffuser into account, and being K the percent of the total lateral area of the diffuser through which the air is supplied.

To have an idea of the range of variation of the governing parameters, Table 2 contains the values used in each simulation together with the case number for future reference.

Simulation	$\dot{V}_s$ (m^3/h)	T_s (ºC)	Re×10^{-4} (-)	Gr×10^{-9} (-)	Γ (-)
case 1	3,500	21	2.8110	4.0460	1.0039
case 2	3,500	22	2.7943	5.4242	1.0073
case 3	3,500	23	2.7777	6.7484	1.0108
case 4	4,000	21	3.2253	3.7485	1.0039
case 5	4,000	22	3.2061	5.1406	1.0073
case 6	4,000	23	3.1871	6.4351	1.0108
case 7	4,500	21	3.6336	3.4422	1.0039
case 8	4,500	22	3.6120	4.8889	1.0073
case 9	4,500	23	3.5905	6.3026	1.0108

Table 2 Different cases simulated

CFD RESULTS

In this section, some results obtained by means of numerical simulations will be presented and discussed. To start with, Figure 6 shows contours of the velocity magnitude in the enclosure. It can be seen that the jet has two clearly differentiated zones: the primary zone, close to the diffuser, where the flow drops to the floor and the velocity increases due to the action of buoyancy forces; and the secondary zone, where the air velocity decreases and the jet maintains a nearly constant thickness. According to previous investigations [32] the separation frontier between primary and secondary zones is defined "as the distance from the diffuser to the point of maximum velocity". For example, this distance is equal to about 2.545 m in case 4, while it is about 2.955 m in case 5. This difference is attributed to the stronger buoyancy forces in case 4 (due to a greater temperature difference between the supply and the enclosure), making the supply air drops faster to floor level. Those stronger buoyancy forces also explain the higher velocity of 0.259 m/s reached in case 4 compared to the maximum velocity of 0.246 m/s reached in case 5.

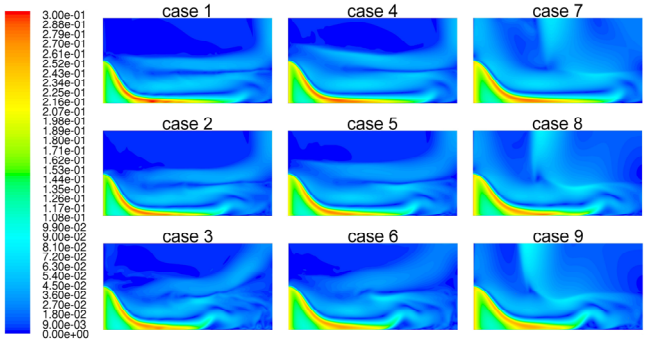

Figure 6 Velocity contours (m/s)

From Figure 6, one can see that the maximum velocity typically occurs near the floor, specifically at heights between 0.05 m and 0.07 m. This result is consistent with literature data [33]. On the other hand, the flow in the vicinity of the floor can be characterized, in a dimensionless way, by the universal profile used for the description of a wall jet flow [34]. In this sense, Figure 7 shows the vertical velocity profiles at different distances from the diffuser in the secondary zone together with the universal wall jet profile. Our velocity profiles are made dimensionless, the velocity with the maximum velocity v_{max} in the profiles, and the z-coordinate with a thickness δ. This length scale δ is defined as the vertical distance where the velocity is half the maximum velocity. The good agreement between all the profiles and the universal one can be understood as a validation of the obtained numerical results.

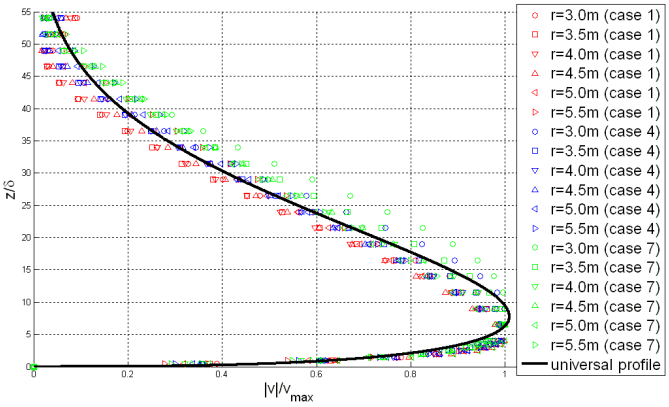

Figure 7 Dimensionless velocity profiles compared with a universal wall jet profile

In addition, Figure 8 represents the maximum velocity (v_{max}) as a function of the radial distance r to the diffuser for three representative cases. This maximum velocity should be proportional to $1/r^n$ where n should be of order unity [35]. As one can see in Figure 8, where the fitting parameters have been included, the agreement with the expected results is quite good.

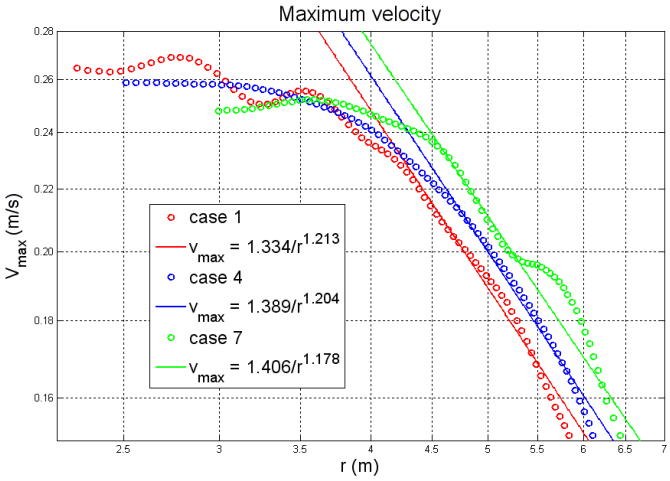

Figure 8 Radial profile of the maximum velocity

In regard to temperature behavior, Figure 9 shows contours of the temperature in the enclosure. A thermally stratified layer is formed due to cold air falling down, and relatively warmer air is at the higher level, causing a vertical temperature gradient. The air temperature within the jet does not vary significantly with the distance from the diffuser.

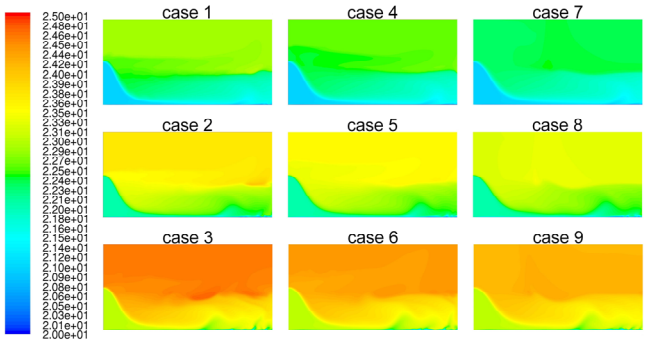

Figure 9 Temperature contours (ºC)

Figure 10 shows profiles in a vertical line when r = 4 m, located in the secondary zone. The vertical temperature gradient is not greater than 2ºC/m, what is consistent with literature data [36]. On one hand, driving a same flow rate (case 1, 2 and 3, see Table 2), air temperature in the enclosure increases when higher supply air temperatures are used. On the other hand, driving air at the same temperature (case 1, 4 and 7, see Table 2), air temperature in the enclosure decreases when higher flow rates are used.

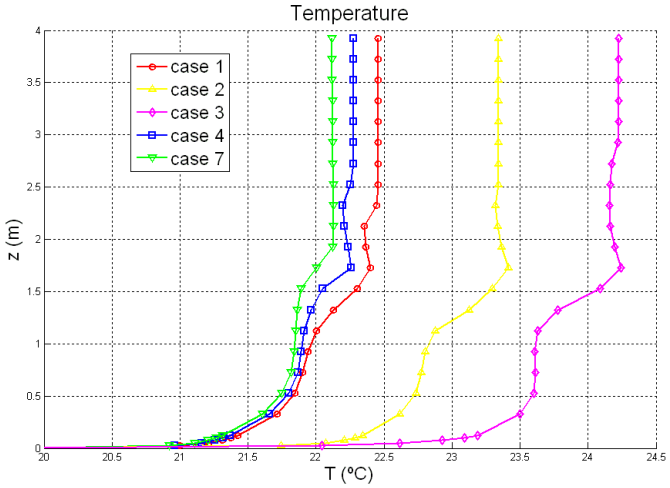

Figure 10 Vertical air temperature profiles

The maximum distance of influence, $D_{influence}$, of the air stream supplied by the diffuser is defined as the radial position where the velocity magnitude drops to a residual value (see Figure 11). This maximum distance of influence is measured along a horizontal line at z = 0.1 m above floor. This height has been chosen because, according to ISO 7730, the discomfort due to vertical thermal gradients is calculated according to air temperature difference between the ankles (0.1 m) and head (1.1 m if the person is seated and 1.7 m if not).

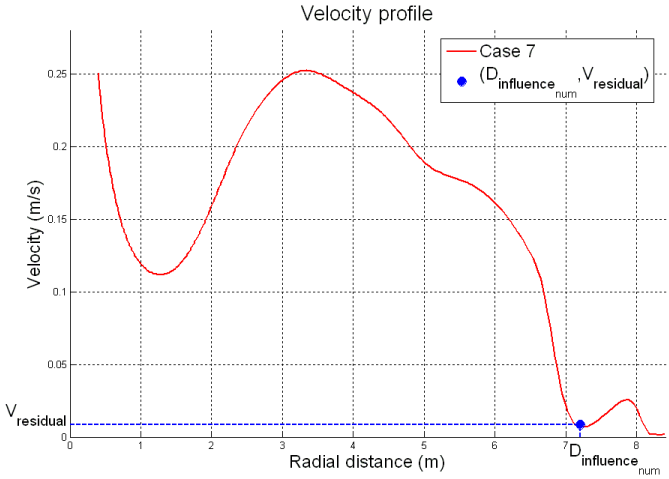

Figure 11 Maximum distance of influence (case 7)

As an example of how this distance is selected, Figure 11 shows the radial profile of the velocity magnitude at z = 0.1 m. The air flow decelerates along the first meter and then accelerates along the next 2 meters, reaching the maximum velocity just when the whole air supplied by the diffuser, due to buoyancy effects, goes down to the ground level, which in case 7 occurs around 3.3 m from the axis of the diffuser. The maximum distance of influence is then chosen after the sharp reduction of the velocity once it vanishes until practically zero, actually until the residual velocity ($v_{residual}$).

In order to have the simplest model of the convective heat flux along the floor, it is going to be modelled as a constant value, q_{const}, in a range of radial lengths between 0.65 m (the radius of the diffuser) and the maximum distance of influence, as shown in Figure 12, where, for a range of radial positions, the heat flux can be considered almost constant, with a value around -1.65 W/m^2 (dashed line) with the radial coordinate varying between 0.65 m and 7.2 m (=$D_{influence}$ in case 7).

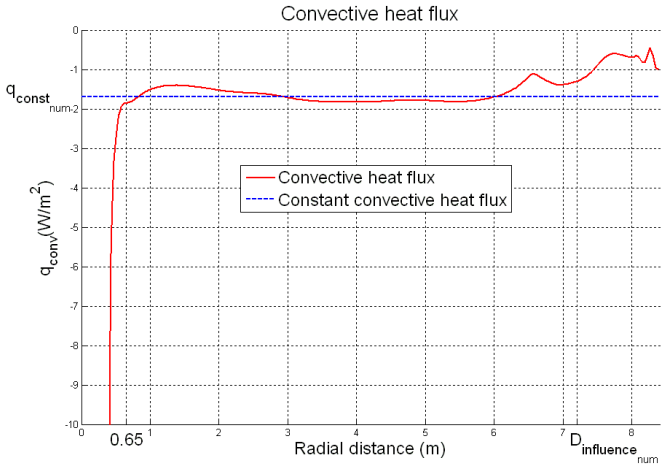

Figure 12 Convective heat flux on the floor (case 7)

The values of the maximum distance of influence and convective heat flux obtained in each simulation were used to obtain, by means of a nonlinear regression, the corresponding

correlations as a function of the dimensionless parameters of the problem. They can be written as

$$D_{influence} = 0.160\, ln\left(Re^{2.396}\, Gr^{1.331}\right) \Gamma^{-54.224}, \quad (6)$$

$$q_{const} = 0.032\, ln\left(Re^{-3.315}\, Gr^{0.218}\right) \Gamma^{137.690}. \quad (7)$$

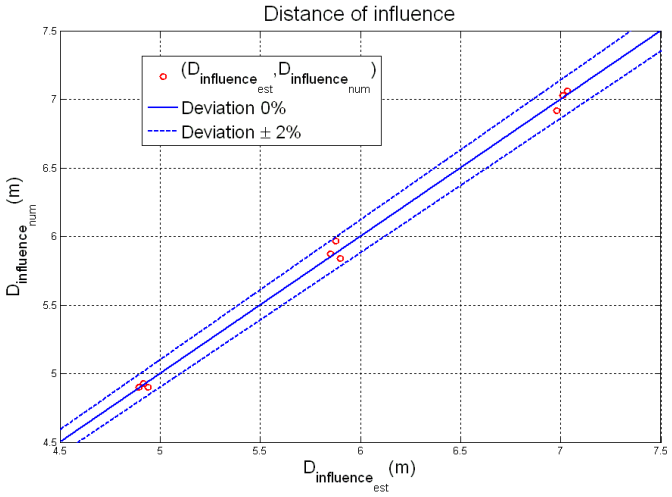

Figure 13 Confrontation of $D_{influence}$ between the applied correlation (6) and numerical values

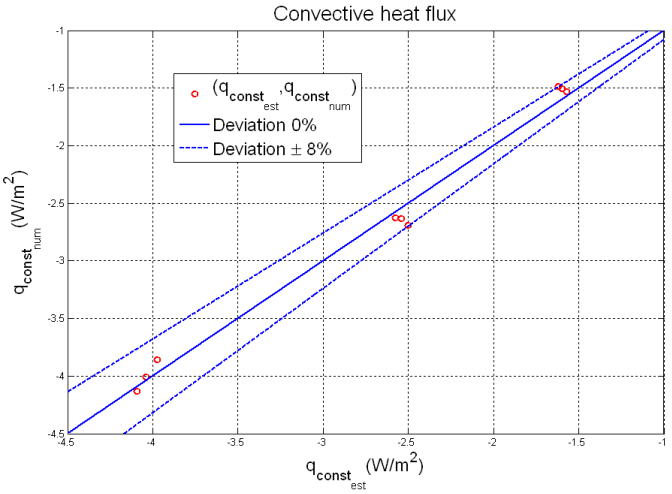

Figure 14 Confrontation of q_{const} between the applied correlation and (7) and numerical values

In what follows, the goodness of the correlations is checked. To that end, the subscripts "est" and "num" are used to name the values estimated by the correlations and those obtained numerically from the simulations, respectively, and both values will be compared. In that sense, Figure 13 shows the maximum distance of influence obtained numerically in the simulations and the value given by the correlation (6) when is evaluated with the dimensionless parameters of the numerical simulations. It can be seen that the errors committed in the estimation are less than 2%. In the same way, Figure 14 compares the convective heat flux estimated by the correlation (7) and that obtained numerically in the simulations. In this case, the errors committed in the estimation are less than 8%.

APPLICATION EXAMPLE

In order to clarify the way the correlations can be used to aid in the dimensioning of a hybrid system (DV+RCF) for cooling purposes, let's imagine the problem of distributing diffusers uniformly in a enclosure similar to that shown in Figure 1, e.g. the boarding area of an airport. This enclosure is characterized by a high solar heat gain on the floor, commonly high rise and high occupancy rates, facts that make it an interesting example for installing the hybrid cooling system proposed. Actually, it is the most common cooling system used in airports throughout the world.

The surface to be cooled is, let's say, about 4,000 m^2 (=A_e), and the cooling system must combat a peak load of 160 kW ($Q_{cool\ peak}$), which is a typical value for south-facing buildings in places with Mediterranean climate. This load also takes into account the thermal loads transmitted through walls, solar radiation, outside air infiltration, occupancy and lighting. Therefore, that load will be the maximum cooling demand, and will be used for sizing the air conditioning system.

The temperature difference between the air exiting the diffuser and indoor air, together with the air flow rate supplied to the enclosure, allow us to calculate the total amount of heat must be combated by the ventilation system, which should be equal to, or higher than, the sensitive cooling load, that is

$$\frac{\dot{V}_t\ \rho\, C_p\ \Delta T_{i\text{-}s}}{3{,}600} \geq Q_{cool\ peak}. \quad (8)$$

The use of a low temperature difference $\Delta T_{i\text{-}s}$ increases the time for "free cooling", contributing significantly to energy saving. Depending on the level of activity of persons, $\Delta T_{i\text{-}s}$ can vary from about 1 ºC to 6 ºC. Therefore, if the air supplied by the diffuser is injected at 21 °C and the temperature in the occupied zone is set to 24.5ºC, the temperature difference is 3.5 ºC. Therefore, the required air flow rate is obtained from equation (8) and is equal, approximately, to 134,000 m^3/h.

Assuming that the selected commercial diffuser has an outer diameter (D) of 0.81 m, a height (h) of 2 m, a percent (K) of 68.5% and supplies an air flow rate ($\dot{V}_s$) of 4,200 m^3/h, therefore, a total of 32 diffusers are needed for injecting the required air flow rate.

Thus, evaluating equations (2), (3) and (4), it follows that the Reynolds number is equal to 4.0978×10^4, the Grashof number is equal to 4.2015×10^9 and the temperature ratio is equal to 1.0034 (which is fixed by the occupancy rate).

On the other hand, it is necessary to ensure that the diffusion of the air injected by the diffuser is able to cover the entire surface of the enclosure. This requires that the influence area of all diffusers, which is calculated according to equation (9), must be greater than the surface of the enclosure, that is

$$A_{influence} = N_d\ \pi \left(D_{influence}\right)^2 \geq A_e. \quad (9)$$

The maximum distance of influence, using equation (2), is 7.3 m, and substituting this value in equation (9) the influence area is equal to 5,357 m^2 (greater than the area of the

enclosure). On the other hand, the convective heat flux along the floor can be obtained using (7) and it is -1.7 W/m^2, where the negative sign indicates that the floor absorbs the heat flux. This value is important in order to adequately dimension the cooling system installed under the pavement.

CONCLUSIONS

The present document delves into the modelling of hybrid cooling systems (composed of ventilation diffusers and a cooling floor) to help in their dimensioning when they are going to be used in large diaphanous enclosures. To that end, a set of numerical simulations have been carried out to obtain a couple of correlations to predict the distance of influence of each diffuser, as well as the heat flux along the floor (considered as constant up to the distance of influence). These correlations depend on the dimensionless governing parameters: Reynolds number; Grashof number and temperature ratio. The proposed correlations have been used in the application example. It has shown how to use them in an enclosure of about 4000 m^2.

ACKNOWLEDGEMENTS

This work has been supported by the company AZVI S.A. (C/ Almendralejo, 5, 41019, Seville, Spain).

REFERENCES

[1] Z. Lin, T.T. Chow, K.F. Fong, Q. Wang, Y. Li. Comparison of performances of displacement and mixing ventilations. Part I: thermal comfort. *International Journal of Refrigeration*, Vol. 28, 2005, pp. 276–287.

[2] Z. Lin, T.T. Chow, K.F. Fong, C.F. Tsang, Q. Wang. Comparison of performances of displacement and mixing ventilations. Part II: indoor air quality. *International Journal of Refrigeration*, Vol. 28, 2005, pp. 288–305.

[3] J.H. Lim, J.H. Jo, Y.Y. Kim, M.S. Yeo, K.W. Kim. Application of the control methods for radiant floor cooling system in residential buildings. *Building and Environment*, Vol. 41, 2006, pp. 60–73.

[4] D. Song, T. Kim, S. Song, S. Hwang, S.B. Leigh. Performance evaluation of a radiant floor cooling system integrated with dehumidified ventilation. *Applied Thermal Engineering*, Vol. 28, 2008, pp. 1299–1311.

[5] X. Jin, X. Zhang, Y. Luo, R. Cao. Numerical simulation of radiant floor cooling system: The effects of thermal resistance of pipe and water velocity on the performance. *Building and Environment*, Vol. 45, 2010, pp. 2545–2552.

[6] F. Causone, F. Baldin, B.W. Olesen, S.P. Corgnati. Floor heating and cooling combined with displacement ventilation: Possibilities and limitations. *Energy and* Buildings, Vol. 42, 2010, pp. 2338–2352.

[7] C.K. Lee, H.N. Lam. Computer modelling of displacement ventilation systems based on plume rise in stratified environment. *Energy and Buildings*, Vol. 39, 2007, pp. 427–436.

[8] G. Smedje, M. Mattsson, R. Walinder. Comparing mixing and displacement ventilation in classrooms: pupils' perception and health. *Indoor Air*, Vol. 21, 2011, pp. 454–461.

[9] H.J. Park, D. Holland. The effect of location of a convective heat source on displacement ventilation: CFD study. *Building and Environment*, Vol. 36, 2001, pp. 883–889.

[10] K.W.D. Cheong, E. Djunaedy, Y.L. Chua, K.W. Tham, S.C. Sekhar, N.H. Wong, M.B. Ullah. Thermal comfort study of an air-conditioned lecture theatre in the tropics. *Building and Environment*, Vol. 38, 2003, pp. 63–73.

[11] C.T. Kiranoudis, K.A. Papakonstantinou, N.C. Markatos. Computational analysis of thermal comfort: the case of the archaeological museum of Athens. *Applied Mathematical Modelling*, Vol. 24, 2000, pp. 477–494.

[12] Q. Li, H. Yoshino, A. Mochida, B. Lei, Q. Meng, L. Zhao, Y. Lun. CFD study of the thermal environment in an air-conditioned train station building. *Buildings and Environment*, Vol. 4, 2009, pp. 1452–1465.

[13] J. Liu, N. Yu, B. Lei, X. Rong, L. Yang Research on indoor environment for the Terminal 1 of Chengdu Shuangliu International Airport. *Eleventh International IBPSA Conference*. Glasgow, Scotland. July 27-30, 2009.

[14] T. Karimipanah, H. B. Awbi, M. Sandberg, C. Blomqvist. Investigation of air quality, comfort parameters and effectiveness for two floor-level air supply systems in classrooms. *Building and Environment*, Vol. 42, No 2, 2007, pp. 647–55.

[15] FLUENT news, Spring 2001.

[16] A. I. Stamou, I. Katsiris, A. Schaelin. Evaluation of thermal comfort in Galatsi Arena of the Olympics ''Athens 2004'' using a CFD method. *Applied Thermal Engineering*, Vol. 8, 2007, pp. 1–10.

[17] C. Y. H. Chao, J. S. Hu. Development of a dual-mode demand control ventilation strategy for indoor air quality control and energy saving. *Building and Environment*, Vol. 39, 2004, pp. 385–97.

[18] E. L. Olsen, Q. Chen. Energy consumption and comfort analysis for different low energy cooling systems in a mild climate. *Energy and Buildings*, Vol 35, 2003, pp. 561–71.

[19] J. Liu, N. Yu, B. Lei, X. Rong, L. Yang. Research on indoor environment for the Terminal 1 of Chengdu Shuangliu International Airport. *Eleventh International IBPSA Conference*. Glasgow, Scotland. July 27-30, 2009.

[20] W. Kessling, S. Holst, M. Schuler. Innovative Design Concept for the New Bangkok International Airport, NBIA. *Symposium on Improving Building Systems in Hot and Humid Climates*. Dallas 2004.

[21] B. W. Olesen. Radiant Floor Heating In Theory and Practice. *ASHRAE Journal*, July 2002.

[22] D. Song, T. Kim, S. Song, S. Hwang, S. B. Leigh. Performance evaluation of a radiant floor cooling system integrated with dehumidified ventilation. *Applied Thermal Engineering*, Vol. 28, 2008, pp. 1299–1311.

[23] P. Simmonds, W. Gaw, S. Holst, S. Reuss. Using radiant cooled floors to condition large spaces and maintain comfort conditions. *ASHRAE Transactions*, Vol. 102, 1996.

[24] Y. Ren, D. Li, Y. Zhang. Numerical simulation of thermal comfort degree in radiant floor cooling room. *Eighth International IBPSA Conference*. Beijing, China. September 03-06, 2007.

[25] X. Yuan, Q. Chen, L. R. Glicksman. A critical review of displacement ventilation. *ASHRAE Trans.* Vol 104, 1998.

[26] M. Deevy M, Sinai Y, Everitt P, Voigt L, Gobeau N. Modelling the effect of an occupant on displacement ventilation with computational fluid dynamics. *Energy and Buildings*, Vol. 40, 2008, pp. 255–264.

[27] ISO 7730:2005. Ergonomics of the thermal environment. Analytical determination and interpretation of thermal comfort using calculation of the PMV y PPD indices and local thermal comfort criteria.

[28] J.M. Peña-Suárez, J. Ortega-Casanova, J.M. Cejudo López. Simulación numérica de difusores de aire para acoplamiento a suelos fríos en grandes recintos. VII Congreso Nacional de Ingeniería Termodinámica. Energía sostenible frente al cambio climático. Bilbao (España). ISBN 84-95416-79-4.

[29] FLUENT 6.3 User's Guide (2006).

[30] V. Yakhot, S.A. Orszag. Renormalization group analysis of turbulence. I. Basic theory. *Journal of Scientific Computing*, Vol. 1, 1986, pp. 3–51.
[31] P. Rohdin, B. Moshfegh. Numerical predictions of indoor climate in large industrial premises – a comparison between different k–ε models supported by field measurements. *Building and Environment*, Vol. 42, 2007, pp. 3872–82.
[32] L. Magnier, R. Zmeureanu, D. Derome. Experimental assessment of the velocity and temperature distribution in an indoor displacement ventilation jet. *Building and Environment*, Vol. 47, 2012, pp. 150-160.
[33] T. Zhang, K. Lee, Q. Chen. A simplified approach to describe complex diffusers in displacement ventilation for CFD simulations. *Indoor Air*, Vol. 19, 2009, pp. 255–267
[34] A. Verhoff. The two dimensional, turbulent wall jet with and without an external free stream. Report Nº 626, Princeton University, Department of Aeronautical Engineering (1963)
[35] P.V. Nielsen. Velocity distribution in a room ventilated by displacement ventilation and wall-mounted air terminal devices. *Energy and Buildings*, Vol. 31, 2000, pp. 179–187
[36] M. Cehlin, B. Moshfegh. Numerical modeling of a complex diffuser in a room with displacement ventilation. *Building and Environment*, Vol. 45, 2010, pp. 2240–2252